Proc. Natl. Acad. Sci. USA
Vol. 82, pp. 7242–7246, November 1985
Biochemistry

Crystal and molecular structure of chymotrypsin inhibitor 2 from barley seeds in complex with subtilisin Novo

(serine proteinase/potato inhibitor 1/molecular replacement method/crystallography)

C. A. McPHALEN*, I. SVENDSEN†, I. JONASSEN‡, AND M. N. G. JAMES*§

*Medical Research Council of Canada Group in Protein Structure and Function, Department of Biochemistry, University of Alberta, Edmonton, Alberta, Canada, T6G 2H7; †Department of Chemistry, Carlsberg Laboratory, Gamle Carlsbergvej 10, DK-2500 Copenhagen Valby, Denmark; and ‡Nordisk Gentofte, N. Steensensvej 1, DK-2820 Gentofte, Denmark

Communicated by Michael G. Rossmann, July 8, 1985

ABSTRACT **The serine proteinase inhibitor from barley seeds, chymotrypsin inhibitor 2 (CI-2), has been crystallized in a molecular complex with subtilisin Novo (EC 3.4.21.14). The crystal structure of this complex has been determined at 2.1-Å resolution by the molecular replacement method and partially refined by restrained-parameter least-squares methods. The present crystallographic *R* factor ($\Sigma||Fo| - |Fc||/\Sigma|Fo|$) is 0.193. CI-2 is a member of the potato inhibitor 1 family; it is a serine proteinase inhibitor lacking disulfide bonds. Comparison of the subtilisin molecule in this complex with the native subtilisin shows that the two molecules are very similar in structure. The inhibitor binds in a mode presumably resembling that of a true substrate, but it is not cleaved. This is in accord with the reported structures of other serine proteinase–inhibitor complexes. CI-2 consists of a four-stranded mixed parallel and antiparallel β-sheet against which an α-helix packs to form a hydrophobic core. A wide loop crossover connection between parallel strands 2 and 3 of the β-sheet contains the reactive-site bond. The conformation of the four residues to either side of the reactive-site bond is similar to that of the analogous residues in the third domain of the turkey ovomucoid inhibitor (Kazal family); the overall polypeptide chain fold of these inhibitors and the location of the reactive site in the respective chains are different.**

Protein inhibitors of the serine proteinases have been grouped into several families based on sequence homologies (1). Members of five of these families have been studied by x-ray crystallography; for some, the structures of both the native state and the enzyme–inhibitor complexes are known. These studies, combined with kinetic and biochemical data, have demonstrated that the inhibitor binds to the enzyme tightly in the manner of a good substrate, but it is cleaved at a very slow rate. The inhibition results primarily from the tight binding and slow release of the inhibitor from the enzyme. In addition, some electrostatic and hydrogen-bonding interactions have been identified (2–4) that may contribute to the slow hydrolysis of the inhibitor by preventing the formation of the required tetrahedral intermediate in the transition state.

Chymotrypsin inhibitor 2 (CI-2), a protein from the seeds of the Hiproly strain of barley, is a member of the potato inhibitor 1 family of serine proteinase inhibitors (5, 6). This family also includes eglin, an inhibitor from the leech *Hirudo medicinalis*. In contrast to most proteinase inhibitors, these two lack stabilizing disulfide bonds; thus, their three-dimensional structures are of interest in determining features that contribute to their stability and inhibitory properties. Crystals of native CI-2 have been reported (7).

The publication costs of this article were defrayed in part by page charge payment. This article must therefore be hereby marked "*advertisement*" in accordance with 18 U.S.C. §1734 solely to indicate this fact.

Subtilisin Novo (EC 3.4.21.14) is a bacterial serine proteinase from *Bacillus amyloliquefaciens*. The structure of the native enzyme has been determined by x-ray crystallography and is similar to that of subtilisin BPN′ (EC 3.4.21.14) (8, 9). The two subtilisins are chemically identical; the two names simply reflect different biological sources. Subtilisin Novo forms a tight 1:1 complex with CI-2 (10).

Two families of serine proteinase inhibitors have been studied extensively by x-ray crystallography: the Kunitz family, which includes pancreatic trypsin inhibitor (11), and the Kazal family, which includes the avian ovomucoid inhibitors (3, 4, 12). Two of the important results from these structural studies are that the reactive-site bonds of these inhibitors are not cleaved in an enzyme–inhibitor complex, and that there is a close approach of the O^{γ} of the active site serine to the carbonyl-carbon atom of the P_1¶ residue of the inhibitor (≈2.7 Å). A tetrahedral enzyme–inhibitor adduct is not formed (1, 14, 15).

We report here the crystal and molecular structure analysis of the complex of CI-2 and subtilisin Novo, refined to a crystallographic *R* factor‖ of 0.193 for the data in the resolution range 6.0–2.1 Å.

MATERIALS AND METHODS

Crystallization. Purified lyophilized CI-2 was prepared in the Carlsberg Research Center, Copenhagen (10, 16), and subtilisin Novo was a gift from Novo Industry (Bagsvaerd, Denmark). CI-2 consists of 83 amino acid residues (Fig. 1) and has a molecular weight of 9250 (17). Subtilisin Novo has 275 amino acid residues and a molecular weight of 27,400 (18).

Plate-like crystals of the complex are grown by the hanging-drop vapor-diffusion method from a solution of 1.4 M $(NH_4)_2SO_4$/50 mM KH_2PO_4, buffered to pH 5.5. The crystals are monoclinic, space group C2. They have unit cell dimensions of a = 103.2(1) Å, b = 56.83(4) Å, c = 68.7(1) Å, and β = 127.4(2)°. The volume per unit molecular weight (V_m) is 2.20 Å^3/Da, consistent with one molecule of the complex (M_r, 36,660) per asymmetric unit and a solvent content of 44% (19).

Data Collection and Processing. X-ray intensity data were collected on a Nonius CAD4 diffractometer. The 2.1-Å data

Abbreviations: CI-2, chymotrypsin inhibitor 2; OMTKY3, third domain of turkey ovomucoid inhibitor; SGPB, *Streptomyces griseus* proteinase B; SSI, *Streptomyces* subtilisin inhibitor.

§To whom reprint requests should be addressed.

¶Nomenclature of Schecter and Berger (13). Amino acid residues of substrates are numbered P_1, P_2, P_3, etc., toward the NH_2 terminus, and P'_1, P'_2, etc., toward the COOH terminus from the reactive-site bond. The complementary subsites of the enzyme binding region are numbered S_1, S_2, etc., and S'_1, S'_2, etc.

‖$R = \Sigma||Fo| - |Fc||/\Sigma|Fo|$, where |Fo| and |Fc| are the observed and calculated structure factors, respectively.

set consisted of 18,705 unique reflections. Corrections were made for absorption (20) (maximum applied factor, 2.09), decay (maximum, 11%), and Lorentz-polarization.

Structure Determination. The method of molecular replacement was used to solve the phase problem for the structure of CI-2 in complex with subtilisin Novo. The search model was the crystal structure of subtilisin BPN', with atomic coordinates from the Brookhaven Data Bank (21), partially refined to an *R* factor of 0.44 at 2.5 Å resolution (22). The rotation search was performed with the fast rotation function (23); the highest peak in the rotation function map, corresponding to the correct solution, was 12.7 σ above the mean and 8.5 σ above the second highest peak. The translation search algorithm was a correlation coefficient search on $|F|^2$. The highest peak in the translation function map was 8.0 σ above the mean.

The coefficients for all electron-density maps used in this structure solution were derived from an expression designed to suppress model bias resulting from phasing by partial structures with errors (R. J. Read, personal communication). The MMS-X interactive graphics system (24) with the macromolecular modeling system M3, developed by C. Broughton (25), was used for map interpretation and model fitting.

Refinement. The restrained-parameter least-squares refinement program of Hendrickson and Konnert (26), modified by Furey (27), and locally by M. Fujinaga for the FPS164 attached processor, was used. After 40 cycles of refinement, the *R* factor was reduced from 0.387 (6.0–2.8 Å resolution) to 0.193 (6.0–2.1 Å resolution). Table 1 summarizes the results for the most recent cycle.

The tracing of the polypeptide chain of CI-2 was completed after cycle 28. The NH_2 terminus of CI-2 is subject to proteolytic cleavage during purification (Fig. 1) (10), and residues 1I–17I may not be present in the complex (an "I" follows the sequence numbers of the inhibitor residues to distinguish them from those of the enzyme). Residues 18I–20I cannot be seen in the current map and may be disordered.

RESULTS AND DISCUSSION

Structure of CI-2. The CI-2 molecule is a wedge-shaped disk of approximate dimensions 28 × 27 × 19 Å, with the reactive-site loop at the narrow end of the wedge. Fig. 2*a* is a drawing of the secondary structural elements in CI-2. In order from NH_2 to COOH terminus, these elements are as follows: strand 1 of the β-sheet, residues Thr-22I–Trp-24I; a type III reverse turn, Trp-24I–Leu-27I; a type II reverse turn, Leu-27I–Lys-30I; 3.6 turns of α-helix, Ser-31I–Lys-43I; a type I reverse turn, Lys-43I–Ala-46I; strand 2 of the β-sheet,

Table 1. Refinement parameters and results for the latest cycle

No. of cycles	40
Resolution range	6.0–2.1 Å
No. of reflections	15,661 [$I \geq \sigma(I)$]
No. of variable parameters	9773
No. of protein atoms	2443
No. of solvent molecules	0
R factor	0.193
rms deviations from ideal values*	
Distance restraints	
Bond distance	0.020 (0.020) Å
Angle distance	0.045 (0.030) Å
Planar 1–4 distance	0.048 (0.040) Å
Plane restraint	0.016 (0.020) Å
Conformational torsion angle	
Planar (ω)	2.7 (3.0)°

*The values of σ, in parentheses, are the input estimated standard deviations that determine the relative weights of the corresponding restraints (26).

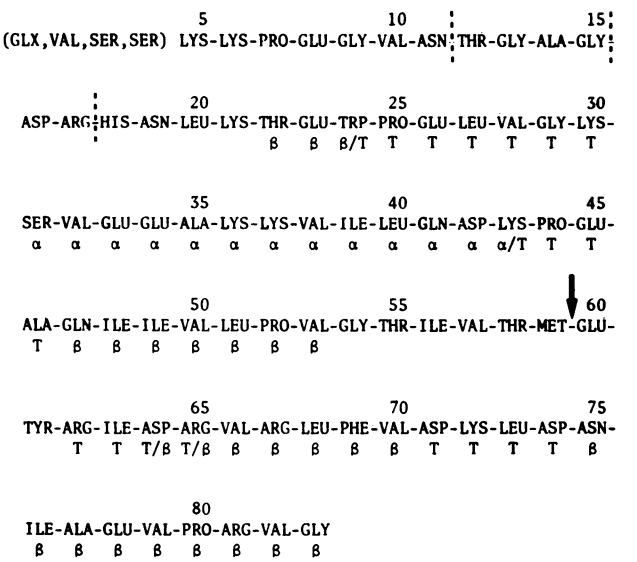

FIG. 1. Amino acid sequence of CI-2. Arrow indicates reactive site. Secondary structural elements are indicated by α (α-helix), β (β-sheet), and T (turn). Vertical dashed lines are known sites of proteolytic cleavage.

Gln-47I–Val-53I; a broad loop, Gly-54I–Tyr-61I, containing the reactive site, Met-59I–Glu-60I; a type I reverse turn, Arg-62I–Arg-65I; strand 3 of the β-sheet, parallel to strand 2, Asp-64I–Val-70I; a type I reverse turn, Asp-71I–Asp-74I; and strand 4 of the β-sheet, antiparallel to strands 1 and 3, Asn-75I–Gly-83I. The four-stranded β-sheet has the characteristic left-handed twist when viewed perpendicular to the strand direction, and the α-helix is packed into the curvature of the sheet with the helix axis aligned to the strand direction. The interface between the helix and the sheet comprises the hydrophobic core of CI-2, composed of residues Trp-24I, Leu-27I, Ala-35I, Val-38I, Ile-39I, Ala-46I, Ile-48I, Val-66I, Leu-68I, Val-70I, Ile-76I, and Pro-80I. The structure of another member of the potato inhibitor 1 family, eglin, from the leech *H. medicinalis*, has been solved in this laboratory in complex with subtilisin Carlsberg (EC 3.4.21.14) (28). The secondary and tertiary structures of eglin are highly similar to those of CI-2.

The Subtilisin–CI-2 Complex. An α-carbon backbone drawing of CI-2 in complex with subtilisin Novo is shown in Fig. 2*b*. Thirteen residues of CI-2 make contacts of <4.0 Å with 24 residues of subtilisin Novo, giving ≈50% more contacts than the complex of the third domain of the turkey ovomucoid inhibitor (OMTKY3) with *Streptomyces griseus* proteinase B (SGPB) (EC 3.4.21.-) (4). The contacts <4.0 Å between CI-2 and subtilisin are summarized in Table 2, and Fig. 3 shows many of these interactions in the active site.

There are far more intermolecular contacts of CI-2 with subtilisin involving residues P_4–P_1 than residues P'_1–P'_3. This is also seen in other serine proteinase–inhibitor complexes (2, 4). Residues Ile-56I–Met-59I (P_4–P_1) form the central strand of a short three-stranded antiparallel β-sheet with Gly-100–Gly-102 and Ser-125–Gly-127 of subtilisin Novo. This interaction is different from that of *Streptomyces* subtilisin inhibitor (SSI, SSI family) with subtilisin BPN' (29). In the SSI–subtilisin complex, residues Gly-102–Tyr-104 form a β-sheet with P_4–P_6; P_2 of SSI is a proline and its imino nitrogen cannot form the hydrogen bond with the carbonyl oxygen of Gly-100 that is seen for Thr-58I of CI-2. In the CI-2–subtilisin complex, the NH of Tyr-104 is too far from the inhibitor to form a hydrogen bond to the CO of Gly-54I (P_6) (Fig. 3). The β-sheet interactions of P_1 and P_3 are similar in the two complexes.

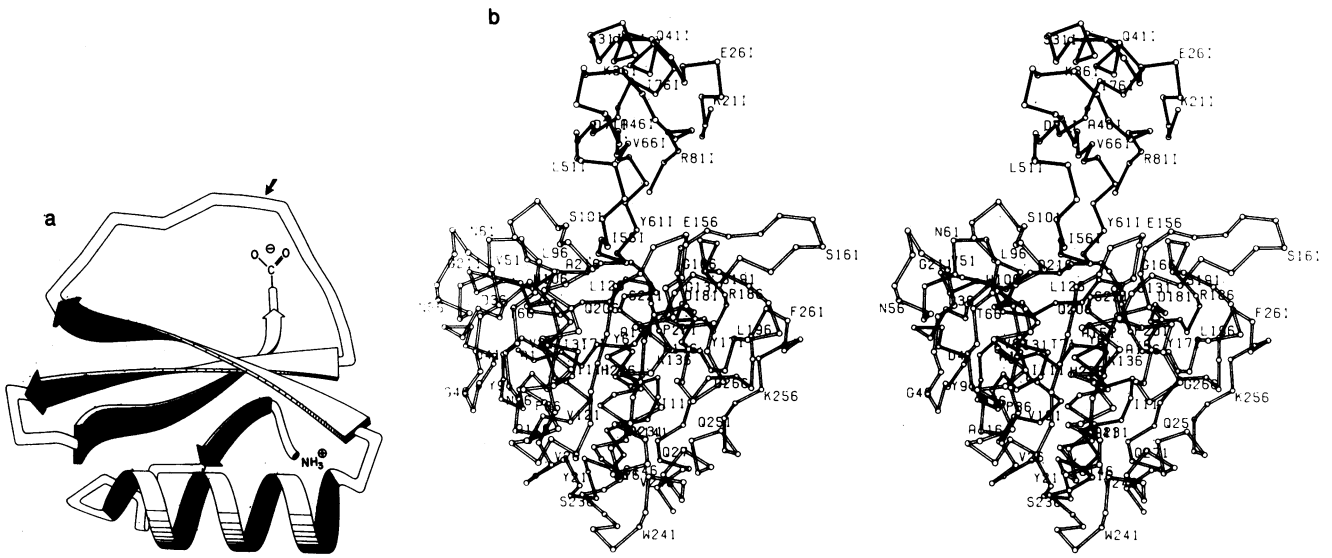

FIG. 2. (*a*) A representation of the secondary structural elements of CI-2. Small arrow at top indicates the reactive site. Large arrows denote β-strands, wide ribbons are α-helix, and narrow ribbons are turns or unclassified structure. (*b*) An α-carbon representation of the CI-2 molecule (filled bonds) in the complex with subtilisin Novo (open bonds). Every fifth amino acid residue is labeled with the residue type and sequence number.

The primary binding pocket in subtilisin, S_1, is very similar to the analogous pocket in α-chymotrypsin (EC 3.4.21.1) (31). The atoms of the main chain segments Ser-125–Gly-127 and Ala-152–Asn-155 form the walls of this pocket (Fig. 3). In addition, the P_1 residue has many contacts with Thr-220–Ser-221. The S_2 binding site in subtilisin is also hydrophobic; the plane of the imidazole ring of His-64 and the side chain of Leu-96 line this region. The side chain of the P_3 residue, Val-57I, points toward the hydrophobic core of CI-2 and makes no direct contacts with subtilisin. The side chain of the P_4 residue, Ile-56I, fits nicely into the S_4 hydrophobic pocket in the enzyme formed by Leu-96, Tyr-104, Ile-107, Leu-126, Gly-127, and Gly-128. P_4 and P_1 account for 48% of all the intermolecular contacts in Table 2.

Table 2. Intermolecular contacts <4.0 Å for subtilisin Novo and CI-2

	Gly-54I P_6	Thr-55I P_5	Ile-56I P_4	Val-57I P_3	Thr-58I P_2	Met-59I P_1	Glu-60I P'_1	Tyr-61I P'_2	Arg-62I P'_3	Σ
His-64					11	1	1			13
Leu-96			1		1					2
Gly-100			1	4	3					8
Ser-101			3	1						4
Gly-102		4	9							13
Gln-103		2								2
Tyr-104	3	2	8							13
Ile-107			3							3
Ser-125					1	4				5
Leu-126			2	3		4				9
Gly-127			3	4		1				8
Gly-128			1							1
Ala-152						2				2
Gly-154						3				3
Asn-155						12	3			15
Phe-189								5		5
Tyr-217									2	2
Asn-218							3	5		8
Gly-219						2		1		3
Thr-220						4				4
Ser-221						12	4			16
Σ	3	8	31	12	16	45	11	11	2	139

An additional 20 enzyme–inhibitor contacts are made by residues Ile-49I, Leu-51I, Glu-78I, and Arg-81I of CI-2 to Asp-99, Ser-101, Pro-129, and Glu-156 of subtilisin. Arg-81I forms an ion pair with Glu-156 (Fig. 3).

On the COOH-terminal side of the scissile bond, the side chain of Asn-155 is within contact distance of the main-chain atoms of Glu-60I, but it is too far away for hydrogen bonding. The NH of Tyr-61I forms a hydrogen bond to the CO of Asn-218; the Tyr-61I side chain stacks with Phe-189 in a hydrophobic interaction. Near the COOH terminus of CI-2 Arg-81I stretches across to form a salt bridge with Glu-156.

In the CI-2–subtilisin complex the "secondary contact region" (29) consists of Ile-49I and Leu-51I side chains with contacts to the enzyme of <4.0 Å. There are no intermolecular hydrogen bonds in this region.

Fig. 4 shows the electron-density map in the region of the active-site residues, Ser-221 and His-64. A difference electron-density map of this region, calculated excluding inhibitor atoms, also shows strong continuous electron density at the scissile bond. This indicates that the inhibitor is uncleaved in the complex. The distance from O^γ of Ser-221 to the carbonyl carbon of Met-59I (P_1) is 2.5 Å, similar to the equivalent distance in other serine proteinase–inhibitor complexes (4). The position of His-64 and Ser-221 relative to the scissile bond of the inhibitor is comparable to that of the analogous residues in the pancreatic-type serine proteinases (3). The NH of Met-59I (P_1) in CI-2 forms a long hydrogen bond of 3.3 Å to the carbonyl oxygen of Ser-125 of subtilisin. This is characteristic of an incipient tetrahedral intermediate (32) and is also observed for OMTKY3–SGPB (3, 4) and for pancreatic trypsin inhibitor–trypsin (EC 3.4.21.4) (11). Part of the stabilization energy for the formation of a tetrahedral intermediate would be obtained by shortening, and thus strengthening, this hydrogen bond.

A least-squares superposition of the 275 α-carbon atoms (program of W. Bennett) in the subtilisin BPN′ model and the subtilisin Novo molecule at refinement cycle 40 gives a root-mean-square (rms) deviation in atomic positions of 0.60 Å. The positions of three α-carbons differ by >2.0 Å: Gly-100, Ser-101, and Gly-102. These residues appear to move toward the active site to form hydrogen bonds with Ile-56I–Thr-58I (P_4–P_2) of the bound inhibitor. Fourteen other residues have α-carbon positions differing by 1.0–2.0 Å.

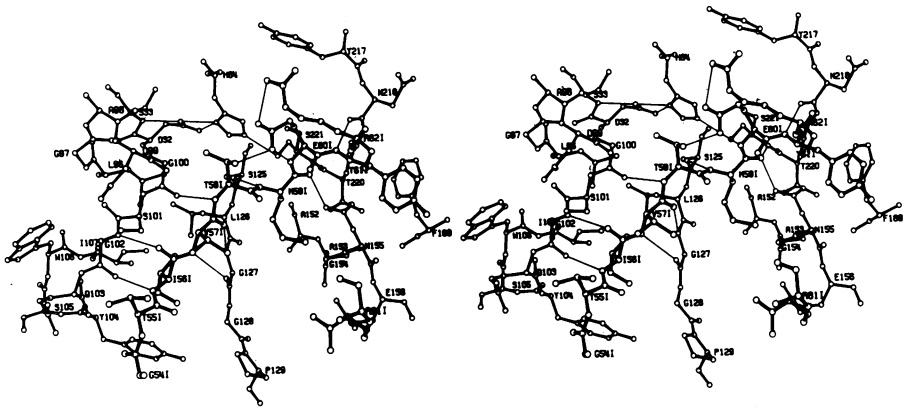

FIG. 3. An ORTEP (30) drawing of the active-site region of subtilisin Novo (open bonds), showing interactions with CI-2 (filled bonds). Hydrogen bonds are indicated by thin lines.

Three of these are close to the Gly-100–Gly-102 loop, and the remainder are in extended loops on the surface of the protein.

Comparison with Other Inhibitors. The sequences around the reactive-site bonds for the potato inhibitor 1, Kazal, SSI, and Kunitz families of serine proteinase inhibitors are very similar (1). Although the homologies in this region are strong, sequence comparisons and x-ray crystallographic studies have shown the remainder of the polypeptide chain to be highly dissimilar among members of different families. The similarity of the reactive-site loops in CI-2 and OMTKY3 (4) can be seen in Fig. 5*a*, as well as the very different chain folding in the remainder of each molecule. A least-squares superposition of main-chain plus C^{β} atoms for residues P_4–P'_3 gives a rms deviation in atomic positions of 2.0 Å. This is a significant difference that is spread along the entire region; whether the source of this difference lies in the interaction of the loop with the cognate enzyme or with the body of the inhibitor may be determinable on further refinement and comparisons.

The relative inflexibility of the reactive-site loop in OMTKY3 is thought to be important to its inhibitory nature (4). This inflexibility results from the two disulfide bridges flanking the scissile bond as well as noncovalent interactions with the body of the inhibitor. CI-2 lacks the stabilizing disulfide bonds, but it appears to have some comparable noncovalent interactions.

The ends of the reactive-site loop are involved in β-structure that wraps around the core of the protein, partly compensating for the lack of disulfide bonds. More importantly, there are two highly conserved arginine residues in the potato inhibitor 1 family; in CI-2 these are Arg-65I and Arg-67I on strand 3 of the β-sheet (Fig. 5*b*). From the conformation and orientation of their side chains, these residues appear to have two functions. First, they act as spacers supporting the reactive-site loop relative to the main body of the inhibitor. In this function, they are analogous to Asn-33I of OMTKY3 and other ovomucoid inhibitors (4, 33). Arginine side-chains are relatively flexible and would allow conformational flexibility in the reactive-site loop for adaptation to different cognate enzymes, in the manner of OMTKY3 adapting to the active sites of SGPB and α-chymotrypsin (34). Second, these two arginine residues are likely involved with the inhibitory mechanism of CI-2 through their hydrogen-bonding and electrostatic interactions with the P_2 and P'_1 residues of the reactive site. Full refinement of the CI-2–subtilisin complex should provide the exact molecular details of these interactions. The positively charged guanidinium groups of the arginines are located similarly to the positive end of a helix dipole in the Kazal inhibitor family. These electrostatic interactions may stabilize the negatively charged side-chains of the P'_1 glutamate or aspartate residues. A more elaborate hydrogen-bonding architecture is present in CI-2 than in OMTKY3, which may also compensate for the lack of disulfide bonds. Interestingly, those inhibitors lacking one arginine—e.g., CI-1 with Phe-67I (6)—are able to inhibit

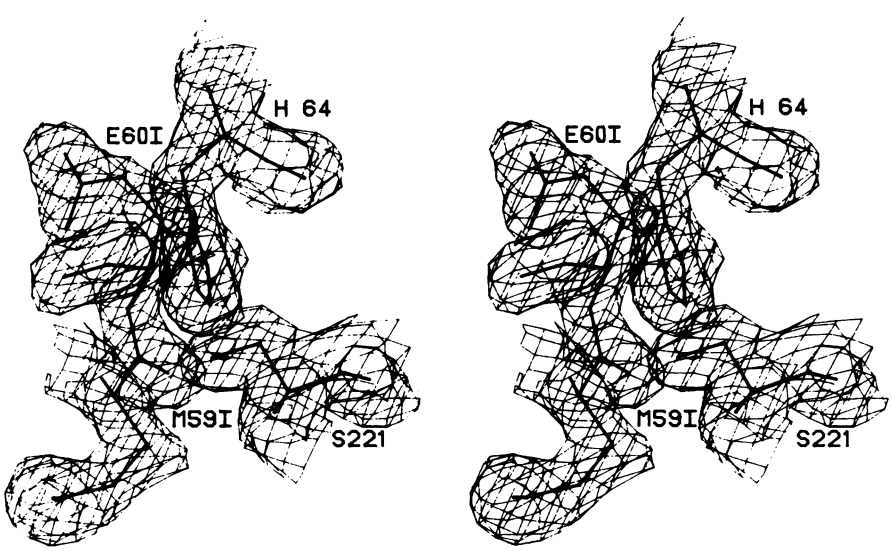

FIG. 4. Electron-density map of the active site of the complex, at refinement cycle 40, calculated with coefficients designed to suppress model bias, and calculated phases. Contour surfaces are drawn at 0.42 $e\text{Å}^{-3}$.

FIG. 5. (*a*) Comparison of the reactive-site regions of CI-2 and OMTKY3. The entire residue is shown for P_4–P'_3 of each inhibitor; an α-carbon representation is given for the remainder of each molecule. Residues P_4–P'_3 of CI-2 are labeled. (*b*) Residues Thr-58I–Arg-67I of CI-2, showing the interactions of Arg-65I and Arg-67I with the reactive-site loop.

subtilisin only temporarily and enzyme activity is regained slowly.

Koto Hayakawa grew the crystals used in this work. We thank Randy Read and Masao Fujinaga for numerous helpful discussions. C.A.M. is the holder of an Alberta Heritage Foundation for Medical Research Studentship. This work was funded by grants to the Medical Research Council of Canada Group in Protein Structure and Function at the University of Alberta from the Medical Research Council of Canada.

1. Laskowski, M., Jr., & Kato, I. (1980) *Annu. Rev. Biochem.* **49**, 593–626.
2. Huber, R. & Bode, W. (1978) *Acc. Chem. Res.* **11**, 114–122.
3. Fujinaga, M., Read, R. J., Sielecki, A., Ardelt, W., Laskowski, M., Jr., & James, M. N. G. (1982) *Proc. Natl. Acad. Sci. USA* **79**, 4868–4872.
4. Read, R. J., Fujinaga, M., Sielecki, A. R. & James, M. N. G. (1983) *Biochemistry* **22**, 4420–4433.
5. Melville, J. C. & Ryan, C. A. (1972) *J. Biol. Chem.* **247**, 3445–3453.
6. Svendsen, I., Boisen, S. & Hejgaard, J. (1982) *Carlsberg Res. Commun.* **47**, 45–53.
7. McPhalen, C. A., Evans, C., Hayakawa, K., Jonassen, I., Svendsen, I. & James, M. N. G. (1983) *J. Mol. Biol.* **168**, 445–447.
8. Drenth, J., Hol, W. G. J., Jansonius, J. N. & Koekoek, R. (1972) *Eur. J. Biochem.* **26**, 177–181.
9. Wright, C. S., Alden, R. A. & Kraut, J. (1969) *Nature (London)* **221**, 235–242.
10. Svendsen, I., Jonassen, I., Hejgaard, J. & Boisen, S. (1980) *Carlsberg Res. Commun.* **45**, 389–395.
11. Marquart, M., Walter, J., Deisenhofer, J., Bode, W. & Huber, R. (1983) *Acta Crystallogr. B* **39**, 480–490.
12. Bode, W., Epp, O., Huber, R., Laskowski, M., Jr., & Ardelt, W. (1985) *Eur. J. Biochem.* **147**, 387–395.
13. Schecter, I. & Berger, A. (1967) *Biochem. Biophys. Res. Commun.* **27**, 157–162.
14. Baillargeon, M. W., Laskowski, M., Jr., Neves, D. E., Porubcan, M. A., Santini, R. E. & Markley, J. L. (1980) *Biochemistry* **19**, 5703–5710.
15. Richarz, R., Tschesche, H. & Wüthrich, K. (1980) *Biochemistry* **19**, 5711–5715.
16. Jonassen, I. (1980) *Carlsberg Res. Commun.* **45**, 47–58.
17. Svendsen, I., Martin, B. & Jonassen, I. (1980) *Carlsberg Res. Commun.* **45**, 79–85.
18. Olaitan, S. A., DeLange, R. J. & Smith, E. L. (1968) *J. Biol. Chem.* **243**, 5296–5301.
19. Matthews, B. W. (1968) *J. Mol. Biol.* **33**, 491–497.
20. North, A. C. T., Phillips, D. C. & Mathews, F. S. (1968) *Acta Crystallogr. A* **24**, 878–884.
21. Bernstein, F. C., Koetzle, T. F., Williams, G. J. B., Meyer, E. J., Jr., Brice, M. D., Rogers, J. R., Kennard, O., Shimanouchi, T. & Tasumi, M. (1977) *J. Mol. Biol.* **112**, 535–542.
22. Alden, R. A., Birktoft, J. J., Kraut, J., Robertus, J. D. & Wright, C. S. (1971) *Biochem. Biophys. Res. Commun.* **45**, 337–344.
23. Crowther, R. A. (1973) in *The Molecular Replacement Method*, International Science Review, ed. Rossmann, M. G. (Gordon & Breach, New York), Vol. 13, pp. 173–178.
24. Barry, C. D., Molnar, C. E. & Rosenberger, F. U. (1976) Technical Memo No. 229 (Computer Systems Laboratory, Washington Univ., St. Louis, MO).
25. Sielecki, A. R., James, M. N. G. & Broughton, C. G. (1982) in *Crystallographic Computing, Proceedings of the International Summer School*, ed. Sayer, D. (Carleton Univ., Ottawa, Oxford Univ. Press, Oxford), pp. 409–419.
26. Hendrickson, W. A. & Konnert, J. H. (1980) in *Biomolecular Structure, Function, Conformation and Evolution*, ed. Srinivisan, R. (Pergamon, Oxford), Vol. 1, pp. 43–57.
27. Furey, W., Jr., Wang, B. C. & Sax, M. (1982) *J. Appl. Crystallogr.* **15**, 160–166.
28. McPhalen, C. A., Schnebli, H. P. & James, M. N. G. (1985) *FEBS Lett.* **188**, 55–58.
29. Hirono, S., Akagawa, H., Mitsui, Y. & Iitaka, Y. (1984) *J. Mol. Biol.* **178**, 389–413.
30. Johnson, C. K. (1965) Report ORNL-3794 (Oak Ridge National Laboratory, Oak Ridge, TN).
31. Robertus, J. D., Alden, R. A., Birktoft, J. J., Kraut, J., Powers, J. C. & Wilcox, P. E. (1972) *Biochemistry* **11**, 2439–2449.
32. Robertus, J. D., Kraut, J., Alden, R. A. & Birktoft, J. J. (1972) *Biochemistry* **11**, 4293–4303.
33. Papamakos, E., Weber, E., Bode, W., Huber, R., Empie, M. W., Kato, I. & Laskowski, M., Jr. (1982) *J. Mol. Biol.* **158**, 515–537.
34. Read, R., Fujinaga, M., Sielecki, A., Ardelt, W., Laskowski, M., Jr., & James, M. N. G. (1984) *Acta Crystallogr. A* **40**, C50–C51 (abstr.).